International Journal of Nanomedicine

Dovepress
open access to scientific and medical research

Open Access Full Text Article

ORIGINAL RESEARCH

Functional design of pH-responsive folate-targeted polymer-coated gold nanoparticles for drug delivery and in vivo therapy in breast cancer

This article was published in the following Dove Press journal:
International Journal of Nanomedicine

Sneha Mahalunkar[1]
Amit Singh Yadav[2]
Mahadeo Gorain[2]
Vinay Pawar[3,4]
Ranveig Braathen[5,6]
Siegfried Weiss[3]
Bjarne Bogen[5,6]
Suresh W Gosavi[7]
Gopal C Kundu[2]

[1]School of Basic Medical Science, Savitribai Phule Pune University, Pune 411007, Maharashtra, India; [2]Laboratory of Tumor Biology, Angiogenesis and Nanomedicine Research, National Centre for Cell Science (NCCS), Pune 411007, India; [3]Institute of Immunology, Hannover Medical School, Hannover, Germany; [4]Department of Molecular Bacteriology, Helmholtz Centre for Infection Research, Braunschweig, Germany; [5]K.G. Jebsen Centre for Influenza Vaccines Research, Institute of Clinical Medicine, University of Oslo, Oslo, Norway; [6]Oslo University Hospital, Oslo 0027, Norway; [7]Department of Physics, Savitribai Phule Pune University, Pune 411007, Maharashtra, India

Correspondence: Gopal C Kundu
Laboratory of Tumor Biology, Angiogenesis and Nanomedicine Research, National Centre for Cell Science (NCCS), Pune 411007, India
Tel +91 202 570 8104
Fax +91 202 569 2259
Email kundu@nccs.res.in

Suresh W Gosavi
Department of Physics, Savitribai Phule Pune University, Pune 411007, Maharashtra, India
Tel +91 202 569 2678
Fax +91 202 569 1684
Email swg@physics.unipune.ac.in

Background: Curcumin has been widely used owing to its various medicinal properties including antitumor effects. However, its clinical application is limited by its instability, poor solubility and low bioavailability. Folic acid (FA)-functionalized nanoformulations may enhance the sustained release of an anticancer drug (curcumin) by tumor-specific targeting to improve therapeutic benefit. This study aims to design a nanoconjugate (NC) comprised of folate–curcumin-loaded gold–polyvinylpyrrolidone nanoparticles (FA–CurAu-PVP NPs) for targeted delivery in breast cancer model systems.

Methods: We developed curcumin-loaded FA-functionalized Au-PVP NCs by layer-by-layer assembly. The folic acid–curcumin Au-PVP NCs (FA–CurAu-PVP NCs) were characterized by ultraviolet–visible spectra, Fourier transform infrared spectroscopy, X-ray powder diffraction and thermogravimetric analysis. In vitro anticancer and antimigratory effects of NCs were examined by performing MTT and wound migration assays. The in vivo antitumor efficacy of NCs was investigated using a preclinical breast cancer orthotopic mouse model.

Results: Curcumin (40 µg/mL) was loaded along with conjugation of folate onto Au-PVP NPs to form FA–CurAu-PVP NCs. The size and charge of the NCs were increased gradually through layer-by-layer assembly and showed 80% release of curcumin at acidic pH. The NC did not show aggregation when incubated with human serum and mimicked an intrinsic peroxidase-like property in the presence of 3,3′,5,5′-tetramethylbenzidine substrate. The MTT data using these NCs showed efficient anticancer activity at lower doses in estrogen/progesterone receptor (ER/PR)-negative cells compared with ER/PR-positive cells. Furthermore, the NCs did not show cytotoxicity at the investigated concentration in human breast epithelial and mouse fibroblast cell lines. They showed inhibitory effects on cell migration and high antitumor efficacy in in vivo analysis.

Conclusion: These results suggest that folate-based tumor targeting using CurAu-PVP NCs is a promising approach for tumor-specific therapy of breast cancer without harming normal cells.

Keywords: curcumin, gold nanoconjugate, folic acid, breast cancer cell line, cytotoxic activity

Introduction

Chemotherapy, although a major treatment, is associated with various side effects as well as poor compliance, and this has boosted significant efforts to find a better anticancer drug modality that uses natural herbal compounds.[1,2] As a result, attempts made by the National Cancer Institute have led to the identification of

natural compounds that exhibit chemopreventive activity.[3] Curcumin, a polyphenol compound isolated from *Curcuma longa* Linn, can sensitize tumor cells by passing through their lipid membrane.[4] Extensive experimental research has clearly shown that native curcumin can modulate molecular targets, thereby inducing cell apoptosis in human tumor-derived cell lines.[5–10] Therefore, we have selected curcumin as a model compound to inform readers about advanced drug-delivery therapies and assist them in exploring other untouched platforms in chemotherapeutic prevention.

The major hurdles in assigning natural compounds such as curcumin as chemopreventives are their low bioavailability, in vivo stability, non-specific biodistribution and non-specific targeting properties. To overcome such issues, various target specific drug-delivery systems have been designed, consisting of nanoparticles loaded with drugs and specific biomarkers, and this is the major area of interest in this particular study.[11,12] Nanocarrier-based delivery systems enable passive targeting due to the leaky vasculature of tumors because of differences in their pore size which enable nanocarriers to target the tumor and accumulate at the tumor site, thereby blunting their effect on normal tissues. Under many circumstances, cancer patients with few other pathophysiological conditions show a non-specific distribution of nanoconjugates to multiple sites which, to some extent, affects the targeting specificity to the tumor zone.[13,14] For this reason, nanocarriers conjugated with drugs can be designed for active targeting using targeting ligands such as folic acid (FA), which can recognize specific receptors overexpressed on certain cancer cell types.

FA is a well-known vitamin for cell proliferation as well as targeting specific biomarkers. FA-functionalized formulations may enhance sustained release of an anticancer drug (curcumin) at the cellular targets to improve the therapeutic benefits. Folate-conjugated nanomaterials have elevated interest in the field of cancer biology, mainly focusing on diagnosis and targeted drug-delivery protocols.[15–17] Salmaso et al formulated targeted delivery by covalently conjugating polyethylene glycol (PEG) to FA at one end of a polymeric carrier which has a cyclodextrin–curcumin complex at the other end. Even though such nanoconjugate complexes entered the clathrin-independent pathway leading to cell endocytosis through targeting overexpressed folate receptors, they showed limited cellular uptake; hence, further investigation is required in terms of drug release efficacy (DRE).[18]

Chemically engineered nanocarriers made up of various materials can be formulated and tuned to act as efficient drug-delivery vehicles. To achieve better targeting and drug release ability, gold nanoparticles (AuNPs) have predominantly been used as nanocarriers.[19] A literature survey showed effective cytotoxic activity of curcumin when it is attached to one of the side chains of soluble polymers such as PEG, polyvinylpyrrolidone (PVP) and chitosan, while the other chain is attached to an AuNP, which also tackles its problems of poor solubility and non-specificity.[20] We have explored FA conjugation and loading of curcumin onto PVP-functionalized AuNPs to target breast cancer cells, which thereby were proven to impart high cell-killing ability. Therefore, a state-of-the-art layer-by-layer (LBL) assembly method for designing nanoconjugates on a solid surface of AuNPs by adsorbing anticancer drug with an oppositely charged polymer such as PVP, involving steric stabilization, is attracting much attention.[21] The LBL assembly can be further enhanced by loading activated folate onto the above-formed conjugate using carbodiimide coupling chemistry. The cross-linking agents that help in forming an amide bond via coupling reactions are 1-ethyl-3-[3-dimethylaminopropyl]carbodiimide (EDC) and dicyclohexylcarbodiimide (DCC). Manju and Sreenivasan demonstrated conjugation of hyaluronic acid with curcumin using DCC/DMAP as a catalyst and coupling agent.[21] The carboxyl group of EDC/N-hydroxysuccinimide (NHS)-functionalized folate can be conjugated with amine-functionalized AuNPs on which the anticancer drug curcumin is loaded, as shown in Scheme 1.[22]

With this background, we hypothesize that we can remove the barriers and limitations associated with classical drug-delivery protocols by encasing an anticancer drug such as curcumin with properties of a multi-drug-resistant modulator and a chemosensitizer on Au-PVP NPs. A target-specific strategy is warranted to enhance the therapeutic efficacy of drug-loaded nanoparticles by conjugating them with extensively investigated epithelial cancer markers such as folate. Thus, our study aims to develop curcumin-loaded FA-functionalized Au-PVP NCs by LBL assembly, which can augment the therapeutic effects and improve the clinical outcomes of curcumin in breast cancer therapy.

Materials and methods

Materials

The chemical and biological compounds used in this research are as follows: folic acid (FA) ($C_{19}H_{19}N_7O_6$),

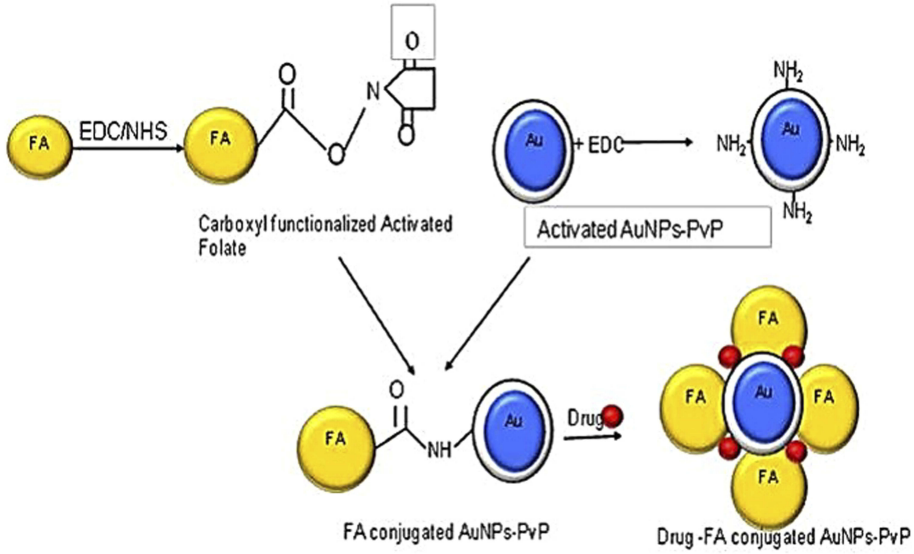

Scheme 1 Schematic representation of folicacid–curcumin–gold–polyvinylpyrrolidone nanoparticles (FA–CurAu-PVP NCs) with layer-by-layer assembly.

N-(3-dimethylaminopropyl)-N-ethylcarbodiimide hydrochloride (EDC.HCl) ($C_8H_{17}N_3$.HCl), N-hydroxysuccinimide (NHS) ($C_4H_5NO_3$) and 3,3′,5,5′-tetramethylbenzidine (TMB) were obtained from Sigma-Aldrich (Bangalore, India). Curcumin crystalline ($C_{21}H_{20}O_6$) was purchased from Loba Chemie (Mumbai, India); acetone, dimethyl sulfoxide (DMSO) and H_2O_2 from Thomas Baker. Chloroauric acid ($HAuCl_4$) and trisodium citrate ($Na_3C_6H_5O_7$) were purchased from SRL and were used as received. Polyvinylpyrrolidone [$(C_6H_9NO)_n$] was collected from CDH. Trypsin/EDTA, penicillin, streptomycin, MTT reagent, propidium iodide, RNase, FBS, DMEM and L-15 media were obtained from Sigma-Aldrich (Bangalore, India). All chemicals were of reagent grade and were used without further purification.

Maintenance of cell lines

Human breast adenocarcinoma (MDA-MB-231 and MCF-7), mouse fibroblast (L929) and human breast epithelial (MCF 10A) cell lines were purchased from American Type Culture Collection (ATCC, Manassas, VA, USA). Mouse mammary carcinoma cell line (4T1) was purchased from Caliper Life Sciences (USA). Cell lines were maintained in L-15 (MDA-MB-231) and DMEM (MCF-7, T47D, 4T1, MCF 10A and L929) supplemented with 10% FBS, 100 units penicillin and 100 µg/mL streptomycin. Cells were subcultured at 70–80% confluence and incubated at 37°C in an incubator supplied with 5% CO_2.

Synthesis of bare AuNPs and PVP-coated AuNPs

Several methods of gold synthesis exist, which produce diverse characteristics in the final product. The method devised by Brust et al[23] showed extensive use of organic phase synthesis concerning a double- or a single-phase process, based on gold salt reduction by sodium citrate as reported by Turkevitch et al,[24,25] which was refined by Frens,[26] who produced spherical size-tunable nanoparticles. The purified AuNPs thus obtained were treated with PVP polymer, which forms a thin covering around the AuNP and can now be used to conjugate with the activated ligands or with another nanoparticle or anticancer agents.

Activation of FA and its conjugation with CurAu NPs to form FA–CurAu-PVP NCs

FA was converted into activated folate to achieve successful conjugation with the amine terminated nanoparticles. The activation of FA was achieved by the previously reported method with few modifications, as follows.[27–29] In brief, 2 mg FA was dissolved in 20 mL DMSO to obtain a clear solution. To the above solution, EDC/NHS (0.4 M/0.1 M) mixture was added, which resulted in activation of COOH groups in FA (Fa/EDC/NHS 2:1:1) and the resulting solution was continuously stirred for about 1 h. Similarly, curcumin (1 mg/mL) was dissolved in acetone and was added in the amine terminated Au-PVP NP solution in a dropwise manner with stirring and heating continuously for 3 h, followed by washing the pellet several

times to remove the traces of unattached curcumin. The activated folate mixture prepared earlier was then added to 5 mL of amine terminated CurAu-PVP NPs solution. The conjugated FA–CurAu-PVP NPs were washed multiple times with deionized water followed by suspending the pellet in PBS. The NC thus formed was stored at 4°C until further use.

Physicochemical characterization of drug-loaded NPs

The functionalized AuNPs were characterized by ultraviolet (UV)–visible spectra (Jasco V-670 spectrophotometer) recorded at 200–800 nm, and Fourier-transform infrared (FTIR) spectra (Jasco FT/IR 6100) were also recorded. The X-ray diffraction (XRD) patterns of curcumin and FA–CurAu-PVP NCs were obtained using a Bruker D8 Advance X-ray diffractometer equipped with Cu Kα radiation source from 10 to 80°C. Thermogravimetric analysis (TGA) was carried out with a Mettler Toledo TGA/DSC 1 Star^e System. FA–CurAu-PVP NCs were also measured by the dynamic light scattering (DLS) technique using a Zetasizer Nano ZS90 instrument (Malvern) with an He-Ne laser beam at a wavelength of 633.8 nm. Transmission electron microscopy (TEM) was used to examine the morphology of the nanosystems (Tecnai G^{2}2).

Determination of drug loading efficiency

The drug loading efficiency (DLE) of curcumin was determined. Curcumin solution was mixed with Au-PVP NPs in a 1:1 ratio and sealed in porous dialysis tube to be dialyzed against PBS (1×, pH 7.4) at room temperature for 24 h. The released drug concentration was monitored by recording UV–visible spectra. The drug loading efficiency was calculated as follows:

$$DLE = (Drug\ loaded\ at\ time\ t\ /\ Total\ drug) \times 100$$

In vitro release of curcumin

Two volumes of 5.0 mL of FA–CurAu-PVP NCs were enclosed in two dialysis bags with a molecular cut-off of 10 kDa and placed separately in two beakers, one containing 150 mL of PBS (1×, blood pH level 7.4) and another with acetate buffer (1×, acidic pH 5.3), with continuous stirring at 100 rpm. At predetermined time intervals, 100 µL of sample was collected and replaced with an equivalent volume of release buffer solution. The released concentration of drug as a function of time was analyzed by UV–visible spectroscopy. The amount of drug released and cumulative release percentage were calculated using the following formula:

$$DRE = (Drug\ released\ at\ time\ t\ /\ Total\ drug) \times 100$$

Colorimetric response of FA–CurAu-PVP NCs

To investigate the peroxidase-mimetic activity of FA–CurAu-PVP NCs, a 1:1 ratio of TMB and H_2O_2 was mixed with 100 µL of 1 µg/mL NC and 0.01 M HNO_3 solution. Next, the mixture of solution was kept at 50°C in a water bath for 30 min and then cooled to room temperature. Subsequently, color change photographs were acquired immediately and UV–visible readings were recorded at 655 nm.

Protein adsorption studies

The UV–visible and FTIR spectra, particle size and zeta potential of NPs can vary after serum protein adsorption or interaction. To evaluate this phenomenon, human serum (HS) was mixed with FA–CurAu-PVP NCs in a 1:1 ratio with a pipette tip to obtain a homogeneous mixture. The mixture was incubated for 22 h at 4°C followed by several steps of washing with deionized distilled water before measurement.

Cell viability assay

The effect of drug-loaded FA–CurAu-PVP NCs on cell viability in breast cancer was evaluated by the MTT assay. In brief, human breast cancer cells (MCF-7 and MDA-MB-231) and mouse breast cancer cells (4T1) were seeded (2×10^4) in a 96-well tissue culture plate. Cells were treated with FA–CurAu-PVP NCs (10, 20, 50, 100 and 200 µg/mL) for 24 h. After 24 h incubation under experimental conditions, the derivatives in the medium were removed and MTT (0.5 mg/mL) was added and incubated for 4 h. Thereafter, the formazan crystals were dissolved in 200 µL of isopropanol and the absorbance was recorded immediately at 570 nm using an automated microplate reader (EPOCH2; BioTek Instruments, Highland Park, VT, USA). Cell viability was analyzed using SigmaPlot 10.0 software. In separate experiments, Human mammary epithelial cells, MCF 10A, and mouse fibroblast cells (L929) were grown in 96-well plates and the MTT assay was performed.

Wound healing assay

The effect of FA–CurAu-PVP on breast cancer cell migration was examined by a wound healing assay. In brief, monolayers of MDA-MB-231 and 4T1 cells were grown in 12-well plates and wounds of uniform size were made with a sterile 10 µL pipette tip. Then, cells were treated with different concentrations of NCs (5–20 µg/mL for MDA-MB-231 and 2.5–10 µg/mL for 4T1 cells) in low-serum media with 4% FBS. Wound photographs were captured at T=0 and T=18 h for MDA-MB-231 cells and at T=0 and T=6 h for 4T1 cells using a phase-contrast microscope (Nikon). The area migrated was quantified (Image-Pro Plus software), analyzed and represented as a bar graph (SigmaPlot 10.0 software).

Determination of cell cycle by flow cytometry

The effect of FA–CurAu-PVP on cell cycle progression in MDA-MB-231 cells was analyzed by fluorescence-activated cell sorting. In brief, MDA-MB-231 cells were seeded in a 60 mm dish at a density of 2×10^5 cells/dish and treated with NCs (20 and 50 µg/mL) for 24 h. After treatment, cells were fixed overnight in 95% ethanol and washed twice in chilled PBS, then the pellet was resuspended in 50 µL of RNase A (0.5 mg/mL) and incubated for 20 min at 37°C. After that, 450 µL of propidium iodide (50 µg/mL) was added. The proportion of cells in different phases of the cell cycle was monitored by a BD FACSCalibur instrument (BD Biosciences).

In vivo antitumor efficacy

All animal experiments were conducted as approved by the Institutional Animal Care and Use Committee (IACUC) of the National Centre for Cell Science (NCCS, Pune, India), in compliance with the 'Committee for the Purpose of Control and Supervision of Experiments on Animals' (CPCSEA) guidelines. 4T1 (1×10^5) cells in a mixture with Matrigel (1:1) (BD Biosciences) were injected into the mammary fat pads of 6-week-old female Balb/c mice. Once tumors had formed, mice were randomly divided into three groups. The first group was left untreated as a control, while the second and third groups were treated intratumorally with curcumin and FA–CurAu-PVP NCs, respectively (10 mg/kg body weight) for 2 weeks. Tumor length and breadth were measured at regular intervals using Vernier calipers. Tumor volume was calculated using the formula:

$$V = \pi/6\left[(lxb)^{3/2}\right]$$

After the required time period, mice were killed and tumors were removed, photographed, weighed and presented graphically.

Statistical analysis

The data are presented as mean ± SEM using SigmaPlot 10.0 software. The level of significance was calculated using the unpaired Student's *t*-test. A p value less than 0.05 ($p<0.05$) was considered statistically significant.

Results

Physiochemical characterization of FA–CurAu-PVP NCs

At the start, AuNPs were synthesized by the Turkevitch method and analyzed by UV–visible spectroscopy. AuNPs were coated with PVP, followed by loading of curcumin on Au-PVP NPs and activation of FA into folate, thereby achieving functionalization of nanoparticles with the EDC coupling reaction, and then conjugating it with activated folate to form FA–CurAu-PVP NCs. The NP thus formed was analyzed and confirmed by UV–visible spectroscopy as well as by FTIR, as shown in Figure 1.

The unmodified AuNPs displayed characteristic surface plasmon absorption at 533 nm; when they were coated with a polymer PVP there was a shift in the peak position (532 nm), suggesting that the AuNPs had been successfully coated with PVP (Figure 1A). The UV–visible spectra for pure FA showed one broad absorption band around 285 nm, corresponding to the л-л* transition of the C–C bond, and another broad shoulder around 364 nm, corresponding to the n-л* transition of the C–O bond in the enone moiety of FA. The spectrum of functionalized FA also showed two broad peaks but with a bathochromic shift from 285 to 312 nm and 364 to 376 nm. Thus, the shift in the spectra of FA before and after functionalization suggests the successful conversion of FA to activated folate (Figure S1). Curcumin-conjugated AuNPs showed a surface plasmon band around 223 nm and 532 nm, suggesting loading of curcumin onto Au-PVP NPs (Figure 1A). This new red peak indicates that curcumin interacted with Au-PVP NPs. Two absorption maxima peaks, at 285 nm and 364 nm, were observed in the UV–visible spectrum of folate-conjugated nanomaterials elsewhere, and the same data can be used to confirm covalent attachment of the folate with AuNPs. Thus, we

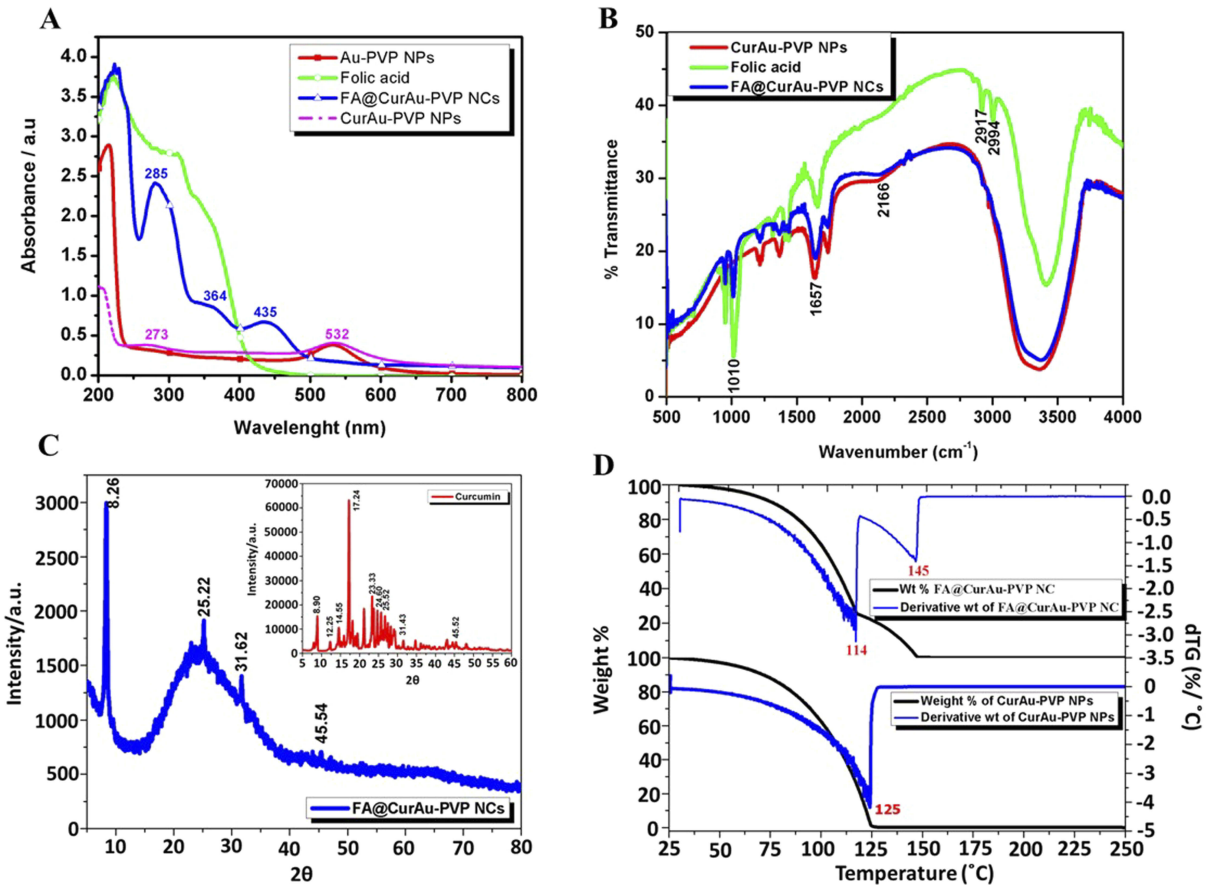

Figure 1 Step-by-step synthesis of folicacid–curcumin–gold–polyvinylpyrrolidone nanoconjugates (FA–CurAu-PVP NCs). (**A**) Ultraviolet–visible spectra of AuNPs and AuNPs coated with PVP. (B) Fourier transform infrared spectra of variation in forming different layers of NCs. (**C**) X-ray diffraction (XRD) spectra of FA–CurAu-PVP NC. Inset: XRD spectra of curcumin. (**D**) DTG result of FA–CurAu-PVP NCs.

observed three major peaks in the FA–CurAu-PVP NC spectrum. Two of these three peaks were at 285 nm and 364 nm, indicating folate covalent bonds, and the other absorption peak was at 435 nm, confirming Au-PVP NP formation, thus suggesting successful bonding of the FA ligand to CurAu-PVP NPs.[30–32] FA–CurAu-PVP NCs showed peaks at 273 nm, 285 nm, 364 nm and 435 nm, respectively. The results also indicate the increase in the size of the sample after modification and conjugation.

Comparing the spectral data of FA and FA–CurAu-PVP NCs shows that both of them had the same unique peaks at 285 nm and 364 nm, which is assigned to the $\pi \rightarrow \pi^*$ transition of the pterin ring of the FA molecule, indicating that FA was successfully conjugated with CurAu-PVP NPs (Figure 1A).[33] To further testify the occurrence and qualitatively analyze conjugation of FA on CurAu-PVP NPs, the nanoconjugates were characterized by FTIR spectroscopy. In the pure FA and functionalized FA, the characteristic peak at 1651 cm^{-1} is accredited to the stretching vibration of –C=O groups. The peaks plotted at 1500–1600 cm^{-1} were the stretching vibrations of C=C determined for the aromatic ring backbone structure.[34] Comparing the infrared spectrum of FA with that of FA–CurAu-PVP NCs, both of them have intensity absorptions plotted at 1429 cm^{-1}, 2911 cm^{-1} and 2999 cm^{-1}. The peak around 1508 cm^{-1} is assigned to N–H bending vibration of the free amine group of folate on FA–CurAu-PVP NCs. When FA was conjugated with CurAu-PVP NPs, a shift in the peak position was noticed with respect to FA, CurAu-PVP NP and FA–CurAu-PVP NCs between 3000 cm^{-1} and 3600^{-1}, which was ascribed to the hydroxyl (OH) stretching bands (Figure 1B). These results suggest successful conjugation of FA on CurAu-PVP NPs to form FA–CurAu-PVP NCs.[34,35] Figure 1C shows the XRD pattern of FA–CurAu-PVP NCs, which reveals a typical amorphous pattern that may be due to AuNPs and a few characteristic peaks of curcumin in the 2θ range of $10 \leq 2\theta \leq 30$ degrees, which indicates the distinct crystalline structure of a hydrophobic drug. Characteristic peaks of curcumin appeared at 8.90, 12.25, 14.55 17.24,

23.33, 24.60 and 25.52 degrees (Figure 1C, inset). Furthermore, the diffraction 2θ peaks observed in the range of 20–30 degrees for curcumin match those in earlier reports.[36–40]

To study the change in sample weight as a function of temperature and to analyze its thermal stability, a very important technique, namely thermogravimetric analysis (TGA), was used. As shown in the thermogram in Figure 1D, CurAu-PVP NPs showed only one step of weight % decrease, while FA–CurAu-PVP NCs showed two steps of weight % decrease. The temperature equivalent to the deep peak at each weight change step is more prominently observed in the first derivative of the TGA curve (DTG) with respect to temperature to obtain a DTG thermogram. The temperature which gives the maximum rate of weight % for a sample (seen as peaks in the DTG thermogram) is considered as the degradation temperature of a component in the material. DTG thermogram of CurAu-PVP NPs showed one step degradation at 125^0C with 99% weight loss which might be the degradation temperature (Td) of curcumin linked Au-PVP NPs whereas after conjugating FA to form FA-CurAu-PVP NCs, temperature at 114^0C and 145^0C showed 95% and 97% weight loss where the second Td might be ascribed to the degradation temperature of folic acid conjugated with CurAu-PVP NPs. The above data also indicate no weight gain in the samples, suggesting that the conjugate was intact without oxidation, and this may be due to the inert nitrogen gas atmosphere. We can thus conclude that the conjugates were successfully formed as FA–CurAu-PVP NCs, which are slightly more stable than CurAu-PVP NPs, and this may be due to layering of FA molecules.

To ascertain the formation of nanoconjugates, we performed DLS and zeta potential measurements and TEM before and after conjugation with the drug curcumin as well as with a biomarker FA, as shown in Table S1. The TEM images showed discrete spherical outlines and monodispersed size distribution (~250 nm) (Figure 2A and B, inset) which were lower values compared with DLS measurements. The nanoconjugate of 250 nm will be ideal for passive tumor targeting as most solid tumors show a vascular cut-off between 380 and 780 nm, as mentioned earlier.[4–11] The DLS result reveals the average hydrodynamic diameter of AuNPs to be 36.85 nm and that of AuPVP to be 62.50 nm. The increase in hydrodynamic size of CurAu-PVP NPs (72.56 nm) compared to PVP-coated AuNPs can be credited to partial cross-linking between the particles during the conjugation process

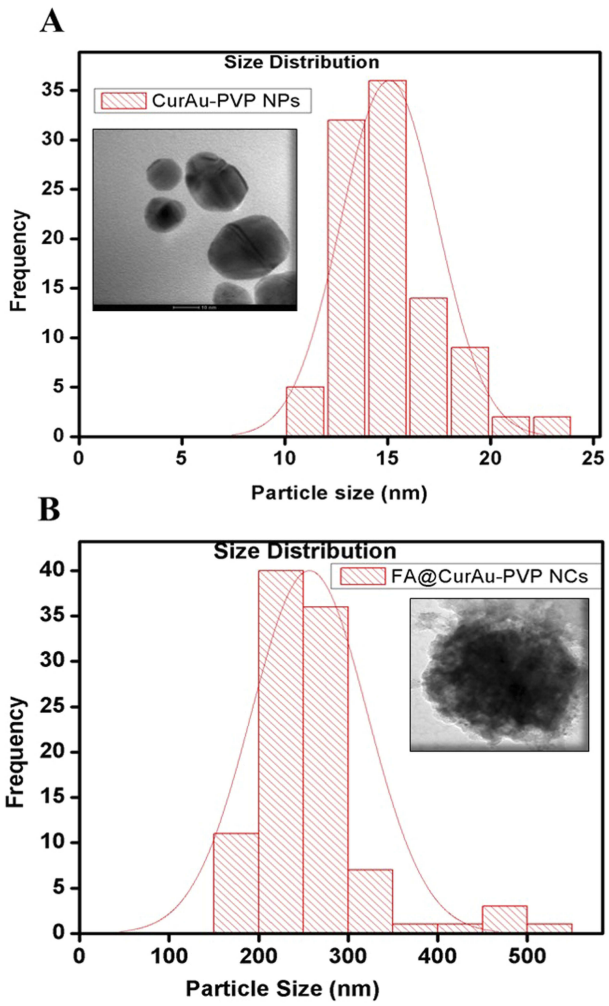

Figure 2 Size distribution and transmission electron microscopy images of (**A**) curcumin–gold–polyvinylpyrrolidonenanoparticles (CurAu-PVP NPs), (**B**) folic acid–curcumin–gold–polyvinylpyrrolidone nanoconjugates (FA–CurAu-PVP NCs).

(Figure 2A),[3] whereas the hydrodynamic diameter of FA-grafted NCs (~358.7 nm) compared to CurAu-PVP NPs with a fairly low polydispersity is consistent with the NHS–folate grafting (Figure 2B).[12] The significant increase in the particle size of the NC formulation can be attributed to the increase in shell volume that resulted from FA incorporation onto the CurAu-PVP NP core.[12] The zeta potential obtained for bare AuNPs was −7.47 mV, which shows a noticeable change after its successful coating with PVP (−9.91 mV) (Table S1). PVP is a neutral and hydrophilic polymer which stabilizes Au-PVP through hydrophilic interaction and therefore is efficiently loaded with hydrophobic oxygen-rich curcumin to form CurAu-PVP NPs.[5] Attachment of partly negatively charged NHS–folate to amine-functionalized CurAu-PVP NPs not only results in increasing negative potential value of FA–CurAu-PVP NCs

but also ensures that the formulations will repel each other to enable long-term storage without particle aggregation.[3–10] Previous reports show that particles with a positive charge favor opsonization followed by reticuloendothelialsystem clearance. Hence, a negative zeta potential of approximately −5 to −20 mV is an appropriate system to arbitrate drug delivery at sites other than the reticuloendothelial system.[8,9] A step-by-step increase in the absolute negative value of the zeta potential of AuNPs with FA–CurAu-PVP NCs by increasing the polymer, drug and folate content indicates that all three components were solubilized not only on the AuNPs but also in the periphery of NCs. The more negative charge of the NC could be also due to the carboxylate group of FA located on the surface of the nanoparticle.[13] The elemental composition from the energy-dispersive X-ray spectroscopy (EDS) spectra shows the maximum percentage of AuNPs and the remainder as C and Cl may be due to polymer, folate and curcumin capping. The EDS spectra of FA–CurAu-PVP NPs reveal the elemental composition of curcumin and FA, with a higher percentage of Ca, H, O and N along with C, Cl and Au proving the successful conjugation of FA and curcumin onto AuNPs (Figure S2).

In vitro drug loading and release studies

The DLE of curcumin was gradual with respect to time and was calculated to be 40 µg/mL of FA–CurAu-PVP NCs, and the DRE in the initial hours (2 h) was found to be 40–45% at blood pH level (pH 7.4) and 80% at acidic pH level (pH 5.3), which were better results than proposed previously (Figure 3A and B).[1] The release profiles at pH 5.3 and pH 7.4 of curcumin are shown in Figure 3C and D. The loaded curcumin was released within a period of 24 h; maximum release was seen within 8 h at pH 7.4 and 6 h at

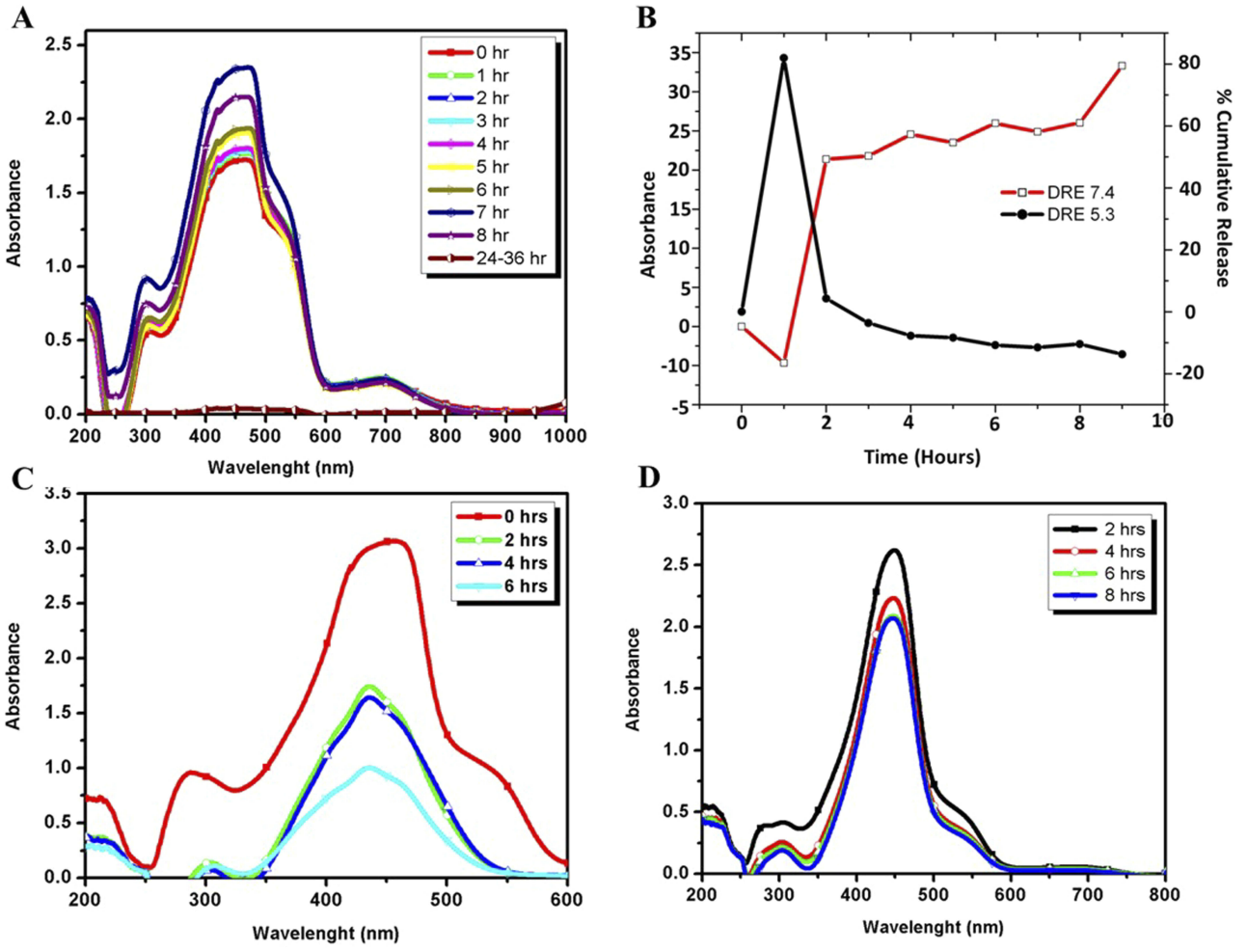

Figure 3 Drug loading and release of curcumin. (**A**) Ultraviolet–visible spectra of drug loading onto the nanoconjugate. (**B**) Cumulative percentage of curcumin released from folic acid–curcumin–gold–polyvinylpyrrolidone nanoconjugates (FA–CurAu-PVP NCs) at pH 7.4 and pH 5.3. (**C**) Curcumin released from FA–CurAu-PVP NCs at pH 5.3. (**D**) Curcumin released from FA–CurAu-PVP NCs at pH 7.4.

pH 5.3, followed by a gradual slow release. This clearly implies that curcumin was loaded successfully onto Au-PVP NPs. Thus, the goal of integrating an anticancer drug (curcumin) onto the nanoparticle, along with FA, to enhance its application in targeted drug-delivery protocols was achieved.

Serum binding studies

Analysis of FA–CurAu-PVP NCs in PBS before and after incubation in HS by UV–visible spectra provided additional evidence about the protein coating. The presence of such a protein coating layer on the nanoconjugates is also known to prevent aggregation of the nanoparticles.[11] Curcumin shows intense absorption from 200 to 450 nm with maximum absorption close to 420 nm. Furthermore, the UV–visible absorption spectra of curcumin bound to HS have a shoulder peak around 450 nm, which is present in the spectra of FA–CurAu-PVP NC as well (Figure 4A).[6] However, in the presence of HS, the curves of absorption of curcumin show striking changes and this may be due to the change in particle size because of protein binding.[3,4] These changes indicate adsorption of serum proteins onto the nanoconjugates. The addition of HS can promote the movement of curcumin from a hydrophilic to a hydrophobic environment, as the aryl groups of curcumin are hydrophobically bound to the hydrophobic pockets of HS.[5] Comparing the spectra of HS alone and when incubated with FA–CurAu-PVP NCs gives information about different types of secondary structures obtained after binding.[4] The FTIR spectra of HS displayed a strong signal at 1645 cm^{-1}, while the spectrum of FA–CurAu-PVP NCs showed changes in the strength and position of the absorption peak between 1600 and 1700 cm^{-1} (Figure 4B). The characteristic amide bands at about 1652, 1542 and 1241 cm^{-1} correspond to C=O stretching, N–H in-plane bending, and C–H stretching as well as C–N and N–H in-plane stretching, respectively (Figure 4B).[9,10] The changes in the band intensity and slight shifts in infrared bands after

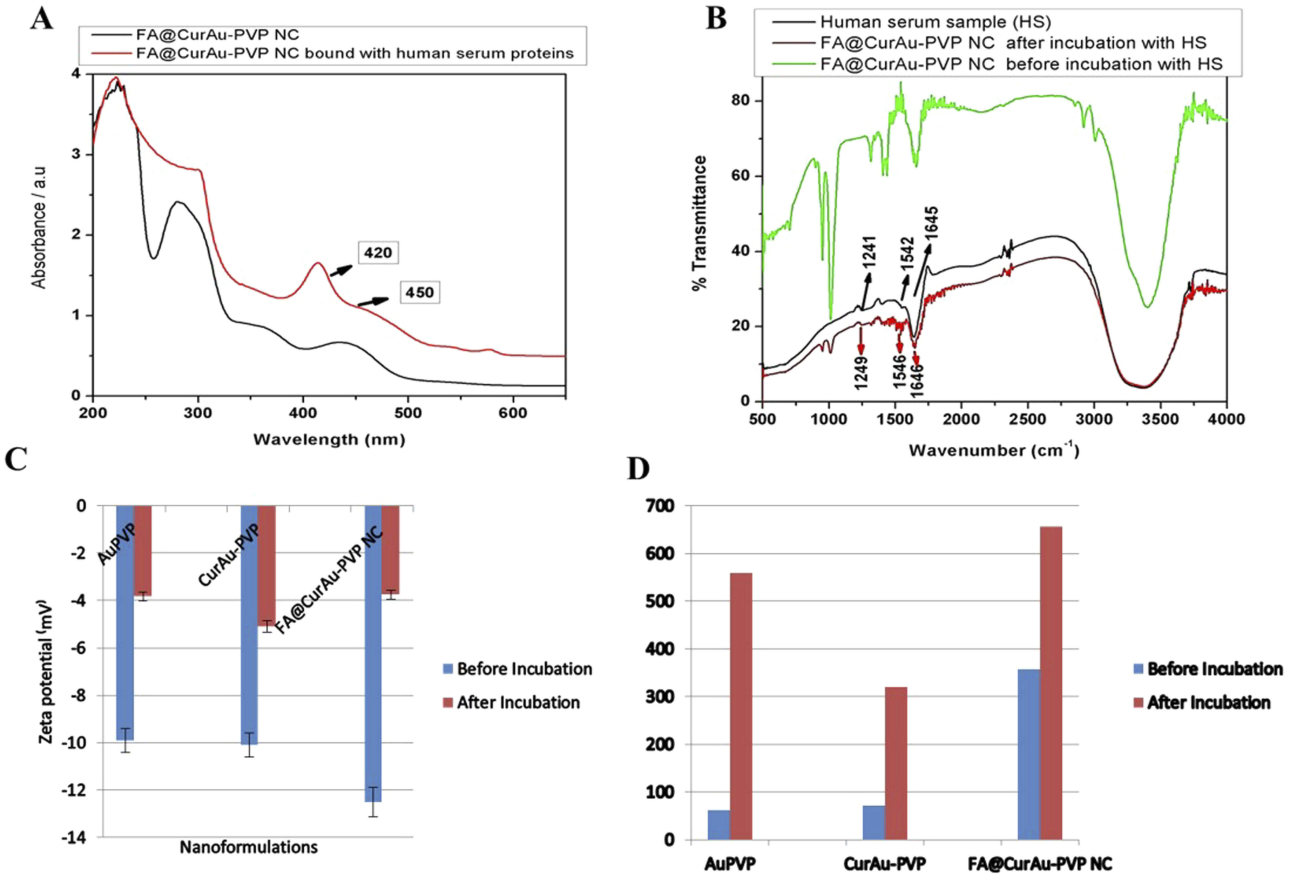

Figure 4 Serum binding studies. (**A**) Ultraviolet–visible spectra of folic acid–curcumin–gold–polyvinylpyrrolidone nanoconjugates (FA–CurAu-PVP NCs) before and after incubation with human serum and (**B**) Fourier transform infrared spectra of naive human serum and FA–CurAu-PVP NCs before and after incubation with human serum. (**C**) Zeta potential measurements of FA–CurAu-PVP NCs before and after incubation with human serum. (**D**) Dynamic light scattering measurements of FA–CurAu-PVP NCs before and after incubation with human serum.

interaction with HS confirm the association of HS proteins to FA–CurAu-PVP NCs. This suggests that by interacting with FA–CurAu-PVP NCs, changes in the secondary structure of HS protein have occurred.

To gain an insight into the HS-induced variation in net surface charge and size of Au-PVP NPs, CurAu-PVP NPs and FA–CurAu-PVP NCs, zeta potential and DLS measurements were carried out under standard experimental conditions. Before incubation of these particles with HS, they were negatively charged. Upon incubation, the mean particle surface charge increased; that is, it became less negative, from −9.91 mV to −3.82 mV for Au-PVP NPs, from −10.1 mV to −5.09 mV for CurAu-PVP NPs and from −12.5 mV to −3.74 mV for FA–CurAu-PVP NPs (Figure 4C and Table S2). HS protein binding to the FA–CurAu-PVP NCs is due to electrostatic effects. Thus, the measured zeta potential of the NC was highly negative before serum incubation and reached neutrality when bound with serum proteins. It can be estimated that there is sequential binding of cationic proteins initially, which may be covering the negative charges on the particles, followed by opsonization of negatively charged proteins to the positively charged protein coat.[3–8] In this study, we also observed an increase in the size of AuNPs when incubated with HS. The adsorbed serum proteins decreased the absolute charge on the particles but increased the size and kept them stable. This stability may be due to Coulombic repulsion between charged particles or to steric hindrance caused by the protein coating, as stated elsewhere.[10] As illustrated in Figure 4D, the size of nanoparticles almost doubles after their incubation with HS, whereas the polydispersity index remains between 0.2 and 0.6, which demonstrates that the nanoparticles are suitable for DLS (Table S2). Thus, DLS was able to detect the increase in size due to enhanced serum protein attachment with the particles.[1] According to previous investigations and the literature, degradation of curcumin has shown that HS acts as an efficient transporter for the curcumin molecule.[7]

Colorimetric assay

To analyze the peroxidase-mimetic activity of FA–CurAu-PVP NCs, the catalytic oxidation of peroxidase substrate TMB in the presence of a catalyst, H_2O_2, was tested. As shown in Figure 5, the AuNPs catalyze TMB substrate oxidation in the presence of H_2O_2 to produce a greenish blue color complex. The maximum absorption peak appeared at 655 nm (Figure 5A). The catalytic activity of NCs is also dependent on the pH of the reaction buffer and incubation temperature. Hence, the pH of the solution (1.0–3.0) and temperature of the reaction system (40–60°C) were optimized in this study. As shown in Figure 5C, the catalytic activity reduced with increasing pH conditions, in the pH range 1–3. Reduced activity was observed in neutral or basic solutions compared to acidic solutions. The best result for a color change from yellow to greenish blue was obtained at pH 1.2 and temperature 50°C, with an HNO_3 concentration of approximately 220–230 µL. TMB has a structure similar to diamine, which leads to a lower solubility in a weak basic medium. Such pH-dependent catalytic activity is mainly associated with the substrates and not with the NCs. On the other hand, the activity elevates with increasing incubation temperature. The experiments showed that the absorbance of FA–CurAu-PVP NCs in the TMB–H_2O_2 system was much higher at pH 1.2, and the same system at pH 1.0 and pH 2.2 showed slight absorbance at 655 nm (Figure 5C). The elevated absorbance at 655 nm is considered to be the gradual increase in the oxidation product of TMB.[3] This result demonstrated that both FA–CurAu-PVP NCs and H_2O_2 were required to catalyze TMB oxidation at standard pH 1.2. Thus, the result also confirmed that FA–CurAu-PVP NCs exhibited an intrinsic peroxidase-mimetic activity, mainly due to the presence of AuNPs in the nanoconjugate. The inset in Figure 5C compares the formation of reaction products against different pH within a time interval of 30 min after the addition of the catalysts (FA–CurAu-PVP NCs and HNO_3) for the color change of TMB. The color change was very fast as soon as the pH was adjusted to 1.2, and after the addition of 0.01 M HNO_3 the change from colorless to greenish blue was observed. The maximum catalytic activity occurred at pH 1.2 and temperature 50°C in the presence of TMB–H_2O_2–FA–CurAu-PVP NCs in the ratio 1:1:1. Therefore, FA–CurAu-PVP NCs show superior peroxidase-like catalytic performance to the peroxidase substrate TMB in the presence of H_2O_2 and under standard pH conditions.[1] Each component separately treated with NC does not give absorbance at 655 nm but the NC with all three components (TMB, H_2O_2 and HNO_3) shows the color change (Figure 5B and D). The AuNPs can catalyze the TMB–H_2O_2 reaction, where H_2O_2 is adsorbed on the surface of AuNPs and the O–O bond of H_2O_2 may be broken up into the double $HO^{\cdot}$ radical.[4,5] Thus, the catalytic ability of AuNP is attributed to the OH radical thus generated. The catalytic efficiency of the NC is strongly dependent on the pH and temperature of the reaction. The 0.01 M HNO_3 was used in the reaction media to

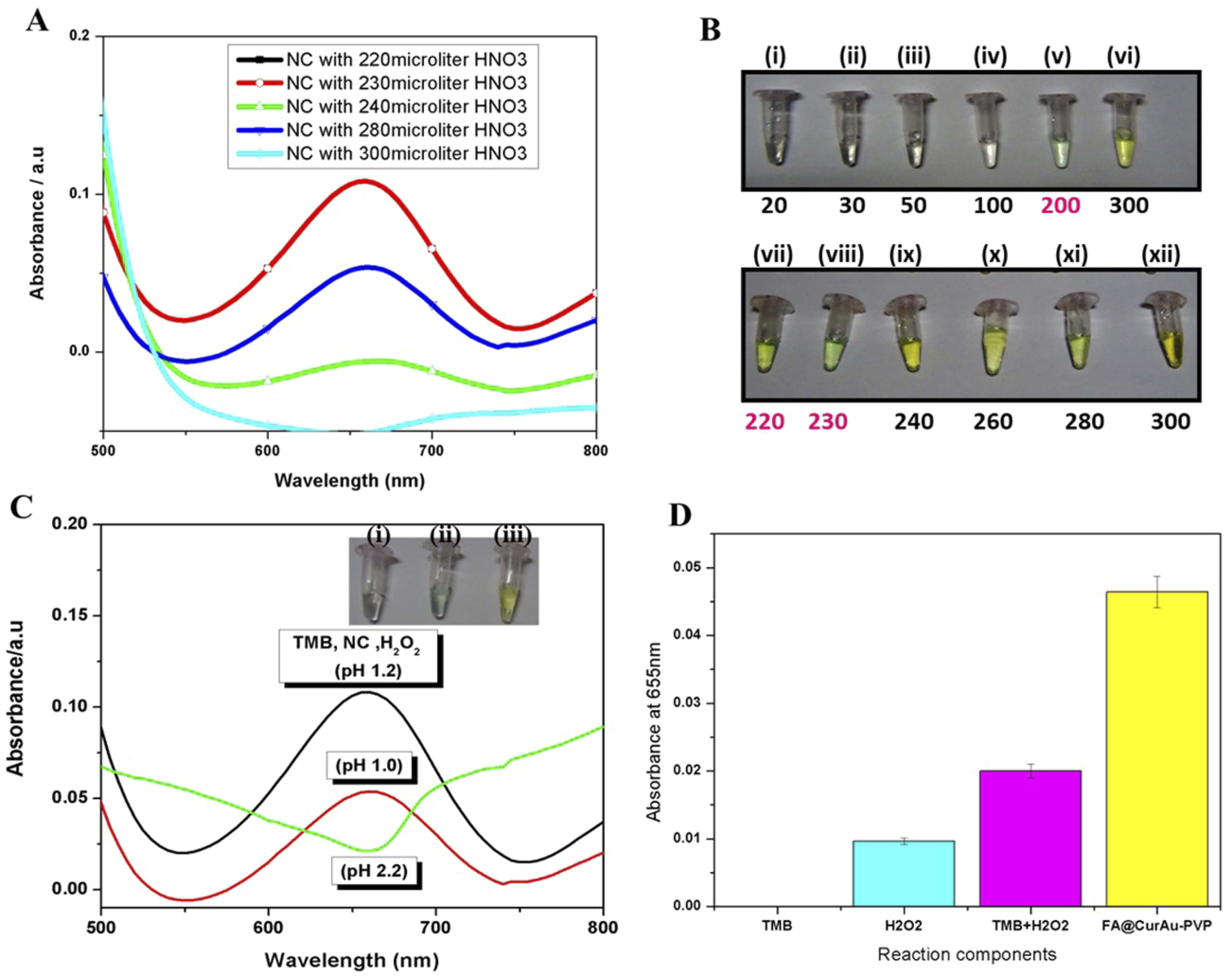

Figure 5 Colorimetric assay. (**A**) Ultraviolet (UV)–visible peaks showing the effect of different concentrations of HNO_3. (**B**) Images illustrating color change after addition of different concentrations of HNO_3: (i) 20 µL, (ii) 30 µL, (iii) 50 µL, (iv) 100 µL, (v) 200 µL, (vi) 300 µL, (vii) 220 µL, (viii) 230 µL, (ix) 240 µL, (x) 260 µL, (xi) 280 µL, (xii) 300 µL. (**C**) UV-visible spectra depicting pH standardization to obtain color change. Inset: Color change at (i) pH 1.0 colorless, (ii) pH 1.2 greenish blue and (iii) pH 2.2 yellow. (**D**) Absorbance at 655 nm of different reaction components: (i) 3,3′,5,5′-tetramethylbenzidine nanoconjugates (TMB-NC), (ii) H_2O_2-NC, (iii) TMB-H_2O_2 and (iv) folic acid–curcumin–gold–polyvinylpyrrolidone nanoconjugates (FA–CurAu-PVP NCs), TMB and H_2O_2.

achieve optimum pH conditions. Thus, the results showed that the catalytic activity was faster in acidic pH solution and this may be due to the presence of enough positive charges on the NCs only in acidic conditions. As tumor tissues have a more acidic environment than normal tissues, this peroxidase-mimetic activity of the NC could be beneficial for intelligent cancer treatments, which would not only kill tumor cells by producing OH radicals but also relieve oxidative stress in normal cells by reducing the H_2O_2 level.[6]

In vitro anticancer activity

To examine the in vitro anticancer activity of NCs, the MTT assay was performed as described previously.[41] Incubation of cancer cells (MDA-MB-231, MCF-7 and 4T1) with the NCs showed the efficient antitumor effect of FA–CurAu-PVP NCs (IC_{50}: 50 µg/mL) in both human and mouse mammary cancer cells (Figure 6A–C). Moreover, incubation of normal cell lines (L929 and MCF 10A) with FA–CurAu-PVP NCs demonstrated low cytotoxicity up to 50 µg/mL dose compared to cancer cells (Figure 6D and E). However, higher doses (100 and 200 µg/mL) showed significant cytotoxicity in both cancerous and normal cells. Hence, the data suggest that NCs can exhibit anticancer activity at low doses without harming normal cells. NCs exhibited a higher inhibitory effect in estrogen receptor (ER)/progesterone receptor (PR)-negative breast cancer cells (MDA-MB-231 and 4T1) compared to ER/PR-positive breast cancer cells (MCF-7). To further confirm our findings, we performed cell-cycle analysis in MDA-MB-231 cells using flow cytometry. The

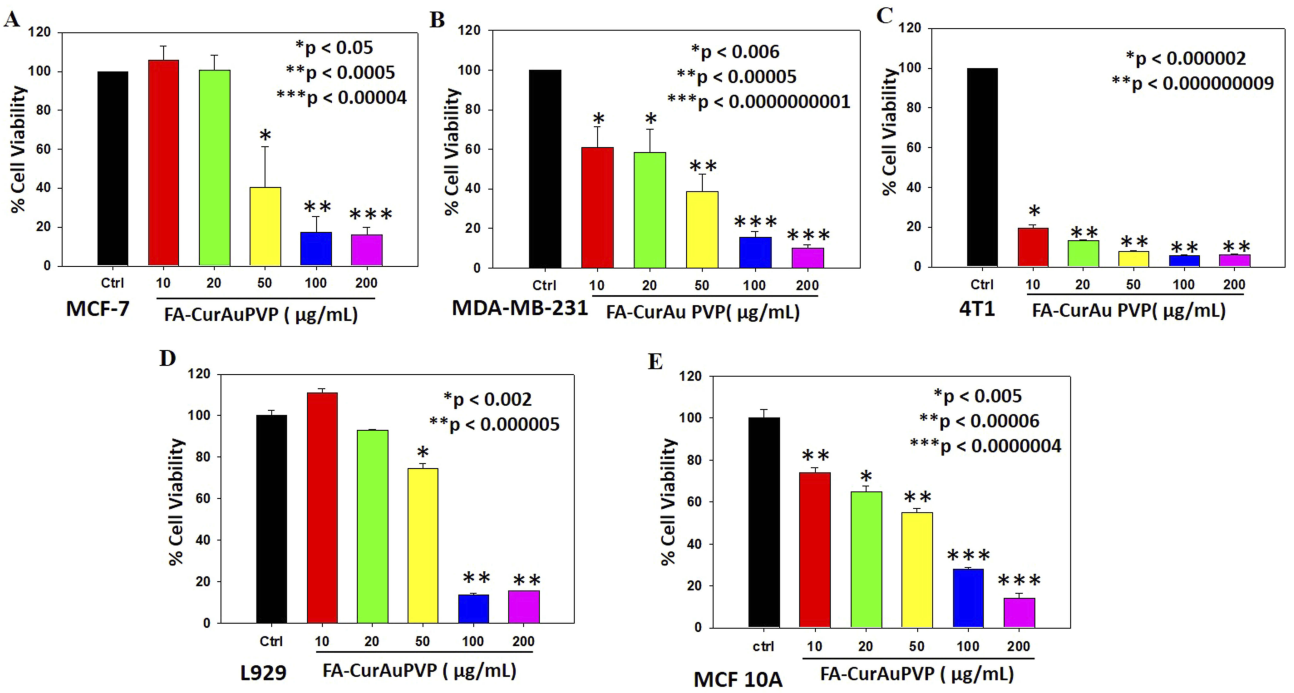

Figure 6 In vitro antitumor effect of folicacid–curcumin–gold–polyvinylpyrrolidone nanoconjugates (FA–CurAu-PVP NCs) in breast cancer. (**A–C**) MCF-7, MDA-MB-231 and 4T1 cells were seeded into 96-well plates and treated with increasing concentrations of FA–CurAu-PVP NCs (0–200 µg/mL) for 24 h. Cell death induced by NCs was analyzed by MTT assay. The percentage inhibition of cell viability is represented graphically. Values are presented as mean ± SEM of three independent experiments, (**D, E**) Mouse fibroblast cells (L929) and Human mammary epithelial (MCF 10A) were seeded into 96-well plates and treated with increasing concentrations of FA–CurAu-PVP NCs (0–200 µg/mL) for 24 h. Cell death induced by NCs was analyzed by MTT assay. The percentage inhibition of cell viability is presented graphically.

data showed an increase in the sub-G_0 population in NC-treated cells compared to controls, suggesting that NC treatment induced cell death (Figure S3).

In vitro antimigratory potential of FA–CurAu-PVP NCs

We further examined the antimigratory property of the NCs in MDA-MB-231 and 4T1 cells. Cells grown in monolayers were wounded and then treated with different concentrations of NCs; they were then observed until a specific time-point at which cell death did not occur. As illustrated in Figure 7, the NCs significantly inhibited migration of 4T1 and MDA-MB-231 cells even at very low doses (Figure 7A and B), proving their antimetastatic potential.

In vivo antitumor efficacy of FA–CurAu-PVP in breast cancer

To examine the antitumor effect of FA–CurAu-PVP NCs under in vivo conditions, 4T1 mouse mammary tumors were generated in Balb/c mice. After tumor generation, mice were treated with free curcumin and FA–CurAu-PVP NCs (10 mg/kg body weight) and the effect on tumor growth was compared with untreated controls. Tumor volumes were measured twice a week by Vernier calipers (Figure 8A). At the end of the experiment, mice were killed; tumors were removed, photographed and weighed (Figure 8A–D). The data demonstrated that FA–CurAu-PVP NCs significantly inhibited the 4T1 breast tumor growth compared to controls. However, at the same dose curcumin did not lead to any significant reduction in tumor growth compared to controls. This may be due to low water solubility, non-specific targeting and early clearance of curcumin from the body. The above findings suggest that FA–CurAu-PVP NCs enhanced the efficacy of curcumin at a dose as low as 10 mg/kg body weight.

Discussion

Nanotechnology has immense potential to produce major advances in areas of enzyme immobilization, energy, food, agriculture and medicine.[42] Nanotechnology-based delivery systems can overcome shortcomings such as drug solubility, permeability and early clearance issues associated with small molecules and drugs, and can provide

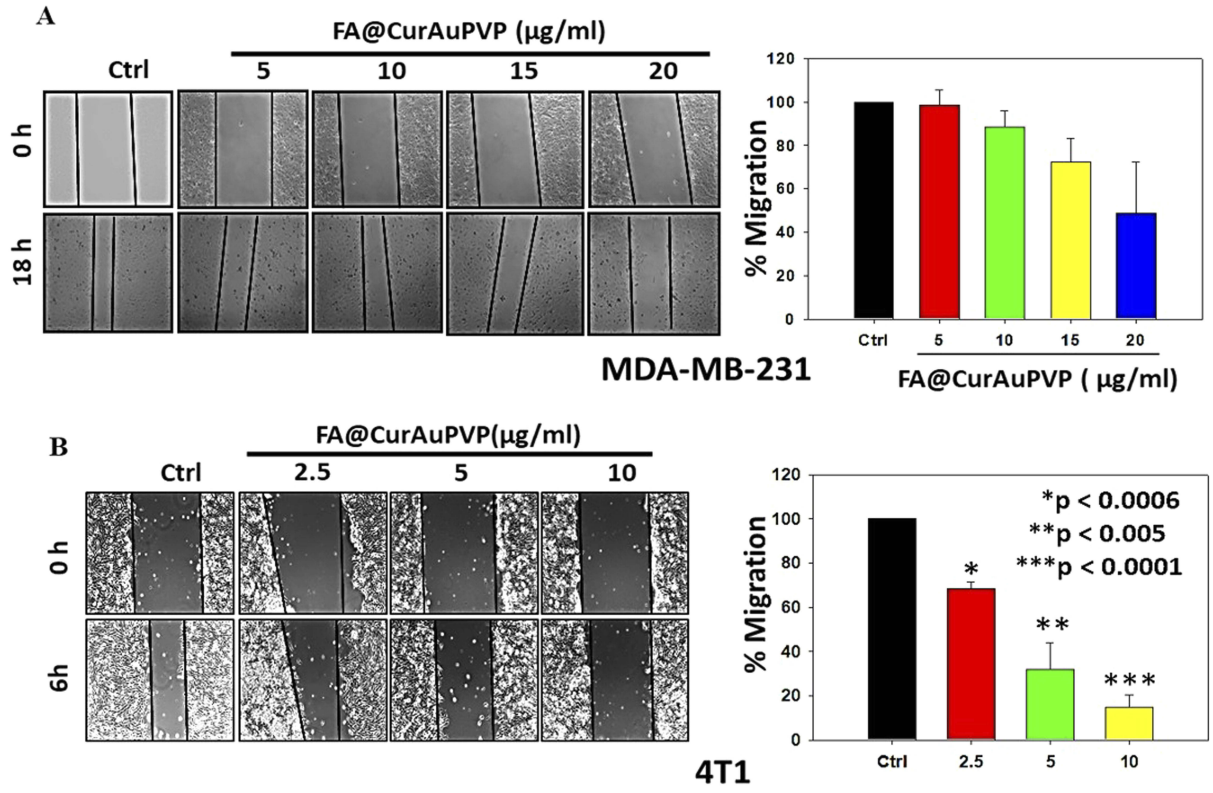

Figure 7 Folic acid–curcumin–gold–polyvinylpyrrolidone nanoconjugates (FA–CurAu-PVP NCs) inhibit migration of breast cancer cells. (**A**) Confluent monolayer of MDA-MB-231 cells wounded with constant width and treated with FA–CurAu-PVP NCs (0–20 µg/mL) for 18 h. Photographs of wounds were taken at T=0 and 18 h. (**B**) Confluent monolayer of 4T1 cells wounded with constant width and treated with FA–CurAu-PVP NCs (0–10 µg/mL) for 6 h. Photographs of wounds were taken at T=0 and 6 h. Migrated distances were measured using Image-Pro Plus software and analyzed statistically and presented graphically using SigmaPlot software. Values are presented as mean ± SEM of three independent experiments.

smart therapeutic solutions such as tissue-specific chemotherapy and phototherapy.[43–46]

In this study, an innovative targeted drug-delivery vehicle (FA–CurAu-PVP NC) with a pH-responsive drug-release system, favorable cytocompatibility and folate receptor-mediated targeting is formulated via a simple covalent cross-linking method for cancer therapy. In the present study, folate-targeted nanoconjugates of CurAu-PVP NPs were synthesized successfully for the delivery of curcumin. Curcumin-loaded optimized FA–CurAu-PVP NCs were spherical, with a mean particle size of approximately 250 nm estimated by DLS and TEM, a zeta potential of −12.5, a narrow size distribution of 0.6 and curcumin DLE of 40 µg/mL. The NCs showed a sustained release behavior during 48 h in two different pH conditions. In this study, we also observed an increase in the size of AuNPs when incubated with HS. The adsorbed serum proteins decreased the absolute charge on the particles and kept them stable, as proven by zeta potential and UV–visible spectra analysis. According to previous investigations and the literature, degradation of curcumin was observed to be reduced in the presence of a serum protein in a buffer solution, which also proves that HS acts as an efficient transporter for the curcumin molecule. FA–CurAu-PVP NCs showed enhanced peroxidase-like activity in the presence of peroxidase substrate TMB with H_2O_2 as a catalyst under a standard pH condition of 1.2.

The MTT assay and flow cytometry studies indicated the higher potential of folate-modified NCs in the inhibition of breast cancer cell proliferation and migration in vitro. Further, the data demonstrated a higher cytotoxicity toward ER/PR-negative compared to positive cells. This may be due to the differential expression of FA receptors on ER/PR-negative and positive cells. It has been reported that there is a higher expression of folate receptors in triple-negative breast cancer, justifying the higher anticancer activity of FA–CurAu-PVP in triple-negative breast cancer cells.[47,48] These findings thereby establish the fact that the synthesized FA–CurAu-PVP NCs showed prominent cytotoxicity in FA receptor-expressing breast cancer cells at doses significantly lower than the doses

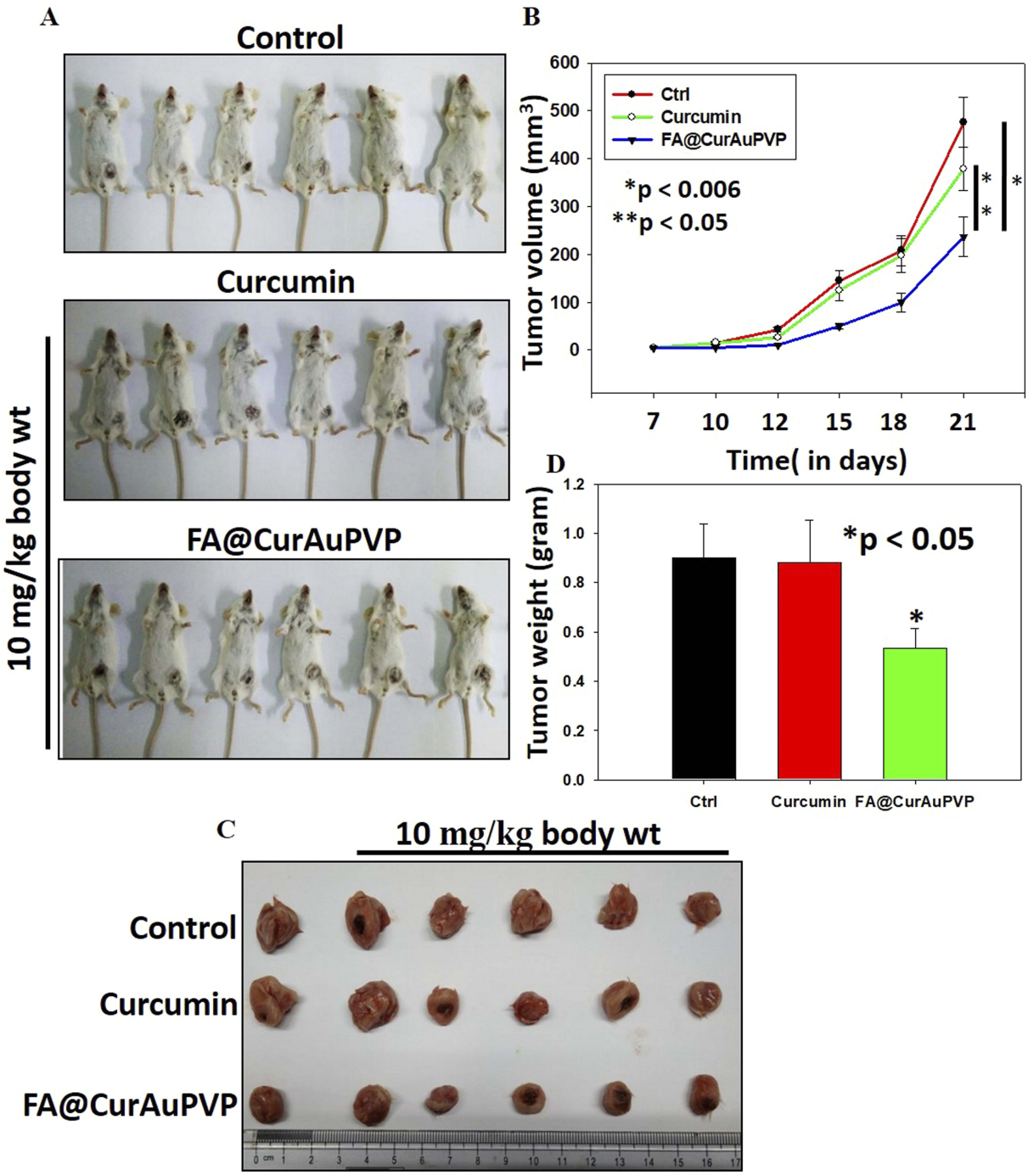

Figure 8 Folic acid–curcumin–gold–polyvinylpyrrolidone nanoconjugates (FA–CurAu-PVP NCs) suppress breast cancer growth under in vivo conditions. (**A**, **B**) 4T1 mouse mammary cells were injected orthotopically into Balb/c mice and then 10 mg/kg body weight of curcumin and FA–CurAu-PVP NCs were injected intratumorally twice a week for 2 weeks. Tumor volumes were measured twice a week using Vernier calipers, analyzed statistically and represented graphically (mean ± SEM, n=5; *p<0.006 compared to control tumor, **p<0.05 compared to curcumin-treated tumor). (**C**, **D**) Tumors were excised, photographed, weighed and analyzed statistically. The bar graph represents mean tumor weights (mean ± SD, n=5; *p<0.05 compared to control).

at which they developed toxicity in normal cells (MCF 10A and L929). The cytotoxic nature of these NCs can also be explained by their enhanced cellular uptake via FA-mediated endocytosis.[5] The ability of cancer cells to undergo migration and invasion has been designated as one of the hallmarks of cancer.[49] During the development of most human cancers, primary cells move out and invade the neighboring tissues and ultimately travel to distant sites to make new colonies, leading to 90% of human cancer deaths. Hence, targeting cancer cell migration and invasion is an important aspect of

cancer chemotherapy.[41,50] Our data showed that FA–CurAu-PVP NCs have excellent antimigratory potential in breast cancer cells. Furthermore, FA–CurAu-PVP NCs significantly inhibited breast tumor growth in an orthotopic mouse model. The enhanced efficacy of curcumin in the present nanoformulation may be the cumulative result of effective tumor targeting through FA receptors and prolonged slow release of the drug at the tumor site. Curcumin also showed higher solubility in the present formulation.

These results suggest that the versatile folate-based tumor targeting using CurAu-PVP NCs is a promising candidate for chemotherapy to kill tumor cells without harming normal cells.

Abbreviations

Au-PVP NPs, gold–polyvinylpyrrolidone nanoparticles; Cur, curcumin; DLE, drug loading efficiency; DLS, dynamic light scattering; ER, estrogen receptor; FA–CurAu-PVP NCs, folic acid–curcumin–gold–polyvinylpyrrolidone nanoconjugates; FA, folic acid; FTIR, Fourier-transform infrared; HS, human serum; NC, nanoconjugate; PR, progesterone receptor; TEM, transmission electron microscopy; TGA, thermogravimetric analysis; TMB, 3,3′,5,5′-tetramethylbenzidine; UV, ultraviolet; XRD, X-ray diffraction.

Acknowledgment

We would like to acknowledge the Department of Science and Technology (DST), Government of India, for providing financial assistance under the project DST/IMRCD/EU/Inno-Indigo/NanoCanTher to carry out this work.

Disclosure

The authors report no conflicts of interest in this work.

References

1. Naksuriya O, Okonogi S, Schiffelers RM, et al. Curcumin nanoformulations: a review of pharmaceutical properties and preclinical studies and clinical data related to cancer treatment. *Biomaterials*. 2014;35:3365–3383. doi:10.1016/j.biomaterials.2013.12.090
2. Ghosh S, More P, Derle A, et al. Diosgenin functionalized iron oxide nanoparticles as novel nanomaterial against breast cancer. *J Nanosci Nanotechnol*. 2015;15:9464–9472. doi:10.1166/jnn.2015.11704
3. Sporn MB, Suh N. Chemoprevention of cancer. *Carcinogenesis*. 2000;21:525–530. doi:10.1093/carcin/21.4.701
4. Fujisawa S, Atsumi T, Ishihara M, Kadoma Y. ROS-generation activity and radical-scavenging activity of curcumin and related compounds. *Anticancer Res*. 2004;24:563–570.
5. Simion V, Stan D, Gan AM, et al. Development of curcumin-loaded poly (hydroxybutyrate-cohydroxyvalerate) nanoparticles as anti-inflammatory carriers to human-activated endothelial cells. *J Nanopart Res*. 2013;15:2108. doi:10.1007/s11051-013-2108-1
6. Anand P, Kunnumakkara AB, Newman RA, Aggarwal BB. Bioavailability of curcumin: problems and promises. *Mol Pharm*. 2007;4:807–818. doi:10.1021/mp700113r
7. Aggarwal BB, Kumar A, Bharti AC. Anticancer potential of curcumin: preclinical and clinical studies. *Anticancer Res*. 2003;23:363–398.
8. Aggarwal BB. Apoptosis and nuclear factor-kappa B: a tale of association and dissociation. *Biochem Pharmacol*. 2000;60:1033–1039. doi:10.1016/s0006-2952(00)00289-6
9. Thangapazham RL, Sharma A, Maheshwari RK. Multiple molecular targets in cancer chemoprevention by curcumin. *Aaps J*. 2006;8:E443–449. doi:10.1208/aapsj080352
10. Manju S, Sreenivasan K. Enhanced drug loading on magnetic nanoparticles by layer-by-layer assembly using drug conjugates: blood compatibility evaluation and targeted drug delivery in cancer cells. *Langmuir*. 2011;27:14489–14496. doi:10.1021/la202470k
11. Roy G, Shetti D, Yadav A, Kundu GC. Nanomedicine: therapeutic applications and limitations. In: Soni S, Salhotra A, Suar M, editors. *Handbook of Research on Diverse Applications of Nanotechnology in Biomedicine, Chemistry, and Engineering*. Hershey: IGI Global; 2015:1–28.
12. Panda JJ, Kaul A, Kumar S, et al. Modified dipeptide-based nanoparticles: vehicles for targeted tumor drug delivery. *Nanomedicine (Lond)*. 2013;8:1927–1942. doi:10.2217/nnm.12.201
13. Gerlowski LE, Jain RK. Microvascular permeability of normal and neoplastic tissues. *Microvasc Res*. 1986;31:288–305. doi:10.1016/0026-2862(86)90018-X
14. Siflinger-Birnboim A, Del Vecchio PJ, Cooper JA, Blumenstock FA, Shepard JM, Malik AB. Molecular sieving characteristics of the cultured endothelial monolayer. *J Cell Physiol*. 1987;132:111–117. doi:10.1002/(ISSN)1097-4652
15. Patel K, Sundara BR, Chen Y, Lou X. Cytotoxicity of folic acid conjugated hollow silica nanoparticles toward Caco2 and 3T3 cells, with and without encapsulated DOX. *Colloids Surf B Biointerfaces*. 2016;140:213–222. doi:10.1016/j.colsurfb.2015.12.046
16. Das M, Sahoo SK, Fatouros D. Folate decorated dual drug loaded nanoparticle: role of curcumin in enhancing therapeutic potential of Nutlin-3a by reversing multidrug resistance. *PLoS One*. 2012;7:e32920. doi:10.1371/journal.pone.0032920
17. Das M, Mohanty C, Sahoo SK. Ligand-based targeted therapy for cancer tissue. *Expert Opin Drug Deliv*. 2009;6:285–304. doi:10.1517/17425240902780166
18. Salmaso S, Barsani S, Semenzato A, Caliceti P. New cyclodextrin bioconjugates for active tumour targeting. *J Drug Target*. 2007;15:379–390. doi:10.1080/10611860701349752
19. Manju S, Sreenivasan K. Gold nanoparticles generated and stabilized by water soluble curcumin–polymer conjugate: blood compatibility evaluation and targeted drug delivery onto cancer cells. *J Colloid Interface Sci*. 2012;368:144–151. doi:10.1016/j.jcis.2011.11.024
20. Manju S, Sreenivasan K. Conjugation of curcumin onto hyaluronic acid enhances its aqueous solubility and stability. *J Colloid Interface Sci*. 2011;359:318–325. doi:10.1016/j.jcis.2011.03.071
21. Manju S, Sreenivasan K. Synthesis and characterization of a cytotoxic cationic polyvinylpyrrolidone-curcumin conjugate. *J Pharm Sci*. 2011;100:504–511. doi:10.1002/jps.22278
22. Biju V. Chemical modifications and bioconjugate reactions of nanomaterials for sensing, imaging, drug delivery and therapy. *Chem Soc Rev*. 2014;43:744–764. doi:10.1039/c3cs60273g
23. Brust M, Walker M, Bethell D, Schiffrin DJ, Whyman R. Synthesis of thiol-derivatized gold nanoparticles in a two-phase liquid-liquid system. *J Chem Soc Chem Commun*. 1994;7:801–802. doi:10.1039/C39940000801
24. Werner S, Arthur F. Controlled growth of monodisperse silica spheres in the micron size range. *J Colloid Interface Sci*. 1968;26:62–69. doi:10.1016/0021-9797(68)90272-5
25. Turkevich J, Stevenson PC, Hillier J. The size and shape factor in colloidal systems. *J Discuss Faraday Soc*. 1951;11:55. doi:10.1039/df9511100055

26. Frens G. Controlled nucleation for the regulation of the particle size in monodisperse gold suspensions. *Nat Phys Sci*. 1973;20:241.
27. Jia CJ, Schuth F. Colloidal metal nanoparticles as a component of designed catalyst. *Phys Chem Chem Phys*. 2011;13:2457–2487. doi:10.1039/c1cp21236b
28. Hyung BE, Young MY, Young-Hwan H. Characteristic optical properties and synthesis of gold-silica core-shell colloids. *Scriptamaterialia*. 2006;55:1127–1129.
29. Wang X, Yao S, Ahn HY, et al. Folate receptor targeting silica nanoparticle probe for two-photon fluorescence bioimaging. *Biomed Opt Express*. 2010;1:453. doi:10.1364/BOE.1.000453
30. Yang H, Zhuang Y, Xiaoxia HHD, et al. Silica-coated manganese oxide nanoparticles as a platform for targeted magnetic resonance and fluorescence imaging of cancer cells. *Adv Funct Mater*. 2010;20:1733–1741. doi:10.1002/adfm.200902445
31. Wu H, Liu G, Zhang S, et al. Biocompatibility, MR imaging and targeted drug delivery of a rattle-type magnetic mesoporous silica nanosphere system conjugated with PEG and cancer-cell-specific ligands. *J Mater Chem*. 2011;21:3037–3045. doi:10.1039/c0jm02863k
32. Zhu Y, Fang Y, Kaskel S. Folate-conjugated Fe3O4–SiO2 hollow mesoporous spheres for targeted anticancer drug delivery. *J Phys Chem*. 2010;114:16382–16388.
33. Zhang Z, Jia J, Lai Y, Ma Y, Weng J, Sun L. Conjugating folic acid to gold nanoparticles through glutathione for targeting and detecting cancer cells. *Bioorg Med Chem*. 2010;18:5528–5534. doi:10.1016/j.bmc.2009.12.033
34. Mine E, Yamada A, Kobayashi Y, Konno M, Liz-Marzán LM. Direct coating of gold nanoparticles with silica by a seeded polymerization technique. *J Colloid Interface Sci*. 2003;264:385–390. doi:10.1016/S0021-9797(03)00422-3
35. Amirthalingam T, Kalirajan J, Chockalingam A. Use of silica-gold core shell structured nanoparticles for targeted drug delivery system. *J Nanomedic Nanotechnol*. 2011;2:119. doi:10.4172/2157-7439.1000119
36. Gangwar RK, Dhumale VA, Kumari D, et al. Conjugation of curcumin with PVP capped gold nanoparticles for improving bioavailability. *Mater Sci Eng*. 2012;32:2659–2663. doi:10.1016/j.msec.2012.07.022
37. Patel A, Hu Y, Tiwari JK, Velikov KP. Synthesis and characterization of zein-curcumin colloidal particles. *Soft Matter*. 2010;6:6192–6199. doi:10.1039/c0sm00800a
38. Dey S, Sreenivasan K. Conjugating curcumin to water soluble polymer stabilized gold nanoparticles via pH responsive succinate linker. *J Mater Chem*. 2015;3:824–833. doi:10.1039/C4TB01731E
39. Anitha VG, Deepagan VV, Divya R, Menon D, Nair SV, Jayakumar R. Preparation, characterization *in vitro* drug release and biological studies of curcumin loaded dextran sulphate-chitosan nanoparticles. *Carbohydr Polym*. 2011;84:1158–1164. doi:10.1016/j.carbpol.2011.01.005
40. Gangware RK, Tomar GB, Dhumale VA, Sharma RB, Datar S. Curcumin conjugated silica nanoparticles for improving bioavailability and its anticancer applications. *J Agric Food Chem*. 2013;61:9632–9637. doi:10.1021/jf402894x
41. Kumar D, Haldar S, Gorain M, et al. Epoxyazadiradione suppresses breast tumor growth through mitochondrial depolarization and caspase-dependent apoptosis by targeting PI3K/Akt pathway. *BMC Cancer*. 2018;18:52. doi:10.1186/s12885-018-4242-8
42. Dwevedi A, Routh SB, Yadav AS, Singh AK, Srivastava ON, Kayastha AM. Response surface analysis of nano-ureases from canavalia ensiformis and cajanus cajan. *Int J Biol Macromol*. 2011;49:674–680. doi:10.1016/j.ijbiomac.2011.06.027
43. Guo B, Zhao J, Wu C, et al. One-pot synthesis of polypyrrole nanoparticles with tunable photothermal conversion and drug loading capacity. *Colloids Surf B Biointerfaces*. 2019;177:346–355. doi:10.1016/j.colsurfb.2019.02.016
44. Wu C, Wang S, Zhao J, et al. Biodegradable Fe (III)–WS2–PVP nanocapsules for redox reaction and TME-enhanced nanocatalytic, photothermal, and chemotherapy. *Adv Funct Mater*. 2019;1901722. doi:10.1002/adfm.v29.26
45. Yang H, Zhao J, Wu C, Ye C, Zou D, Wang S. Facile synthesis of colloidal stable MoS2 nanoparticles for combined tumor therapy. *Chem Eng J*. 2018;351:548–558. doi:10.1016/j.cej.2018.06.100
46. Prasad R, Chauhan DS, Yadav AS, et al. A biodegradable fluorescent nanohybrid for photo-driven tumor diagnosis and tumor growth inhibition. *Nanoscale*. 2018;10:19082–19091. doi:10.1039/c8nr05164j
47. Necela BM, Crozier JA, Andorfer CA, et al. Folate receptor-α (FOLR1) expression and function in triple negative tumors. *PLoS One*. 2015;10:e0122209. doi:10.1371/journal.pone.0122209
48. Zhang Z, Wang J, Tacha DE, et al. Folate receptor α associated with triple-negative breast cancer and poor prognosis. *Arch Pathol Lab Med*. 2013;138:890–895. doi:10.5858/arpa.2013-0309-OA
49. Hanahan D, Weinberg RA. Hallmarks of cancer: the next generation. *Cell*. 2011;144:646–674. doi:10.1016/j.cell.2011.02.013
50. Yadav AS, Pandey PR, Butti R, et al. The biology and therapeutic implications of tumor dormancy and reactivation. *Front Oncol*. 2018;8:72. doi:10.3389/fonc.2018.00072

Supplementary materials

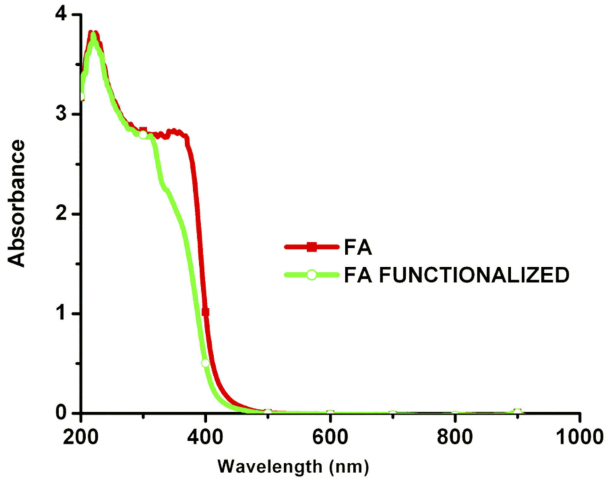

Figure S1 UV-Visible spectra representing activation of folic acid in o folate.

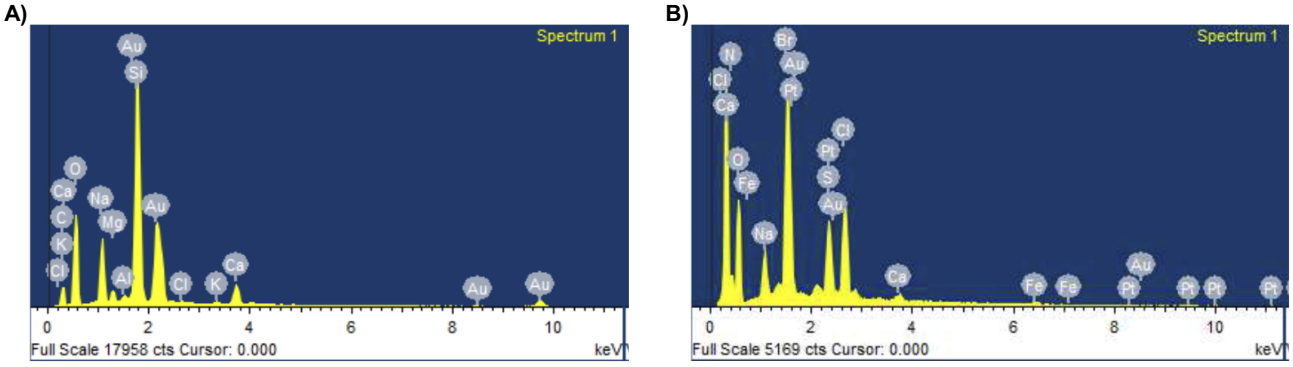

Figure S2 (**A**) EDS graph of AuNP, (**B**) EDS graph of FaCur @AuNC.

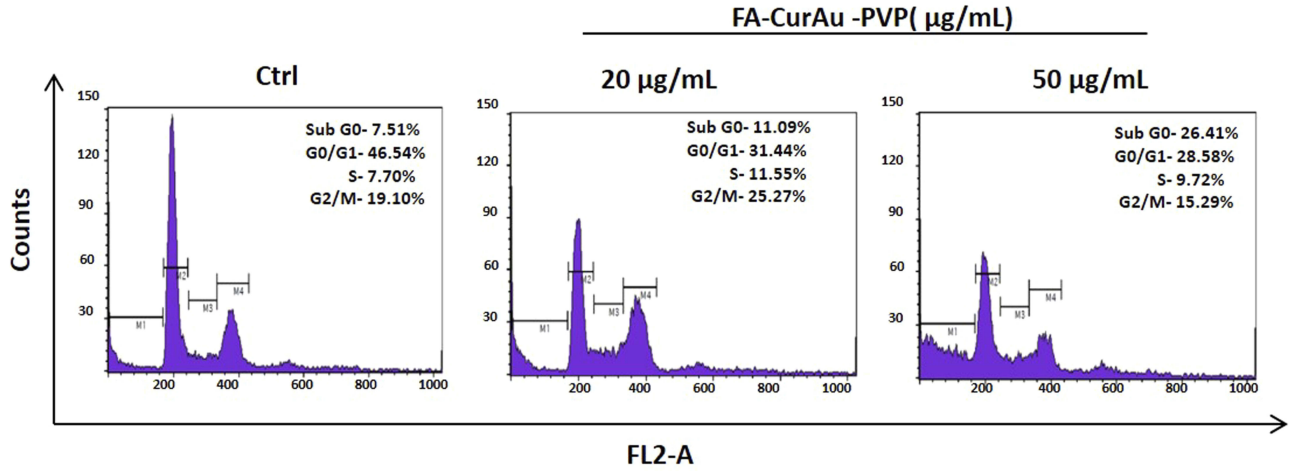

Figure S3 Effect FA@CurAu-PVP treatment on cell cycle in MDA-MB-231 cells was analyzed by flow cytometry. Briefly, 2×10^5 cells were seeded in 60 mm dish and treated with 20 and 50 µg/ml of FA@CurAu-PVP for 24 hrs. Cells were stained with propidium iodide and analyzed by FACSCalibur (BD Bioscieces).

Table S1 Hydrodynamic size (D_h), polydispersity index (PDI) and zeta potential of gold nanoparticles (AuNPs) and successively functionalized AuNPs, curcumin–gold polyvinylpyrrolidone nanoparticles (CurAu-PVP NPs) and folic acid–curcumin gold–polyvinylpyrrolidone nanoparticles (FA–CurAu-PVP NPs) at physiological pH

Sr. no.	Formulation	D_h (nm)	PDI	Zeta potential (mV)
1	AuNP	36.85	0.296	−7.47
2	AuPvP	62.50	0.338	−9.91
3	CurAu-PVP NP	72.56	0.582	−10
4	FA–CurAu-PVP NC	358.7	0.6	−12.5

Table S2 Summary of size (dynamic light scattering), polydispersity index (PDI) and charge of gold–polyvinylpyrrolidone (Au-PVP) functionalized nanoparticles (NPs), curcumin–gold (CurAu NPs) and folic acid–curcumin gold (FA–CurAu) NPs before and after incubation with human serum

Formulation	DLS: hydrodynamic diameter (nm)	PDI	Zeta potential (mV)
Au-PVP NPs before incubation	62.5	0.338	−9.91
Au-PVP NPs after incubation	559	0.239	−3.82
CurAu NPs before incubation	72.5	0.582	−10.1
CurAu NPs after incubation	320	0.393	−5.09
FA–CurAu NPs before incubation	358	0.6	−12.5
FA–CurAu NPs after incubation	657	0.393	−3.74